Electronic Supplementary Information (ESI)

Kinetic model facilitates analysis of fibrin generation and its modulation by clotting factors: implications for hemostasis-enhancing therapies

by Alexander Y. Mitrophanov, Alisa S. Wolberg, and Jaques Reifman

Abbreviations

AP, α_2-antiplasmin; APC, activated protein C; AT, antithrombin; FDP, fibrin degradation products; Fg, fibrinogen; FnI, fibrin I monomers; FnII, fibrin II monomers; FPA, fibrinopeptide A; FPB, fibrinopeptide B; FII, prothrombin; FIIa, thrombin; FVa5, FVa3, and FVa53, partially proteolyzed forms of factor (F)Va; HCF and LCA1, inactive FVa fragments; mIIa, meizothrombin; PAI, plasminogen activator inhibitor 1; PC, protein C; Pg, plasminogen; Pn, plasmin; TAFI, thrombin-activatable fibrinolysis inhibitor; TFPI, tissue factor pathway inhibitor; Tm, thrombomodulin; tPA, tissue-type plasminogen activator.

Kinetic model description

Our mechanistic model of thrombin generation, fibrin formation, and fibrinolysis consists of 80 coupled, nonlinear ordinary differential equations (ODEs) for the biochemical species and reactions listed in Table S1, and one algebraic equation that accounts for TAFI effects (see *Representation of TAFI effects*). Model parameters are also listed in Table S1, and the initial conditions are shown in Table S2. Each ODE defines the rate of change in the concentration of a biochemical species involved in the blood clotting process. We followed the standard approach of biochemical kinetics, with the total rate of change for a species concentration expressed as a sum of all production and depletion rates corresponding to the chemical reactions in which that species participates.

The model was implemented in the SimBiology package of the MATLAB R2012a software suite (MathWorks, Natick, MA). Model equations were solved with numerical integration parameters chosen as described in Mitrophanov and Reifman [1]. All computations were performed in MATLAB R2012a.

Representation of TAFI effects

Our representation of TAFI effects was based on the following considerations. First, we found that the empirical dependency of relative clot lysis time on [TAFI] (Fig. 3*B,* squares) can be accurately approximated via the function

$$\mathrm{LT}_{\mathrm{relative}}(\mathrm{TAFI}) = \frac{a[\mathrm{TAFI}]}{1 + b[\mathrm{TAFI}]} + 1, \qquad \text{(S1)}$$

where the constants a and b were determined by fitting the function to the data using MATLAB's `cftool` environment. Next, we used the finding that lysis time (LT) is approximately inversely proportional to [tPA] (see Ref. [2]), as follows. Assume that LT_0 is the

LT for a pre-formed clot in the absence of TAFI in a system where fibrinolysis is triggered by tPA (at a concentration [tPA]). If we add TAFI (at a concentration [TAFI]) to the system, then LT will increase. If LT_{TAFI} denotes the new LT value, then it follows from Eq. S1 that

$$\frac{LT_{TAFI}}{LT_0} = \frac{a[TAFI]}{1+b[TAFI]} + 1. \quad (S2)$$

We could increase LT in the same system in the absence of TAFI by reducing the concentration of tPA. Indeed, for a new tPA concentration, $[tPA]_{new}$,

$$\frac{LT_{new}}{LT_0} = \frac{[tPA]}{[tPA]_{new}}, \quad (S3)$$

where LT_{new} is the new LT value [2]. This argument implies that we could change [tPA] in the TAFI-free system in such a way that the resulting relative LT change would be equal to LT_{TAFI}/LT_0 from Eq. S2. We will denote the corresponding new tPA concentration as $[tPA]_{TAFI}$. Combining Eqs. S2 and S3, we obtain

$$\frac{a[TAFI]}{1+b[TAFI]} + 1 = \frac{[tPA]}{[tPA]_{TAFI}}$$

and, therefore,

$$[tPA]_{TAFI} = [tPA] \Big/ \left(\frac{a[TAFI]}{1+b[TAFI]} + 1 \right).$$

This is the equation used in our model to account for TAFI effects by adjusting the initial tPA concentration in the ODE system representing the reactions in Table S1. However, the dependency of LT on [tPA] in our model somewhat deviates from strict inverse proportionality, which can be illustrated by the deviation of the dependency of LT on 1/[tPA] from a straight line (Fig. S5). To account for this deviation, we adjusted the constant *a* by multiplying it by a factor of 0.8. The final values of *a* and *b* are 5.222×10^8 M^{-1} and 2.676×10^8 M^{-1}, respectively. These values were used with the model to generate the results shown in Fig. 3 (solid lines).

Parameter selection

Many of the model's parameter values were taken directly from original works published by experimental groups (Table S1, footnote). In the case of thrombin–antithrombin complex formation rate (k_{41}), we had to choose between two values from different publications, i.e., 7.1×10^3 $M^{-1}\cdot s^{-1}$ reported by Hockin et al. [3] and 1.6×10^4 $M^{-1}\cdot s^{-1}$ reported by Naski and Shafer [4]. We chose the latter, which resulted in a better match with the benchmark experimental data on prothrombin titration (Fig. 2*A*). While k_{57}, the rate of antiplasmin binding with plasmin, may depend on the concentration of fibrin degradation products, our model gives a simplified description of this process as a binding reaction with a single rate constant, whose value is within the possible range determined from available measurements [5].

Some of the parameters were adjusted from their original values to improve the model's fidelity. The catalytic rate of plasminogen activation (k_{59}) was increased by 1.55 fold from its original value given in Ref. [6] (we used the plasminogen activation parameter values reported

there for [Glu[1]]plasminogen). This allowed our model to better capture the benchmark experimental data on fibrinogen titration in Fig. 2*B*. The rate constants k_{78} and k_{79} were increased and decreased, respectively, by 3 fold compared with their original values in Ref. [7]. This further improved the correspondence between the model output and the benchmark fibrinogen titration data (Fig. 2*B*).

The values for parameters k_{61}−k_{77} and k_{80} were initially taken directly from Ref. [7]. However, the resulting model (with all the other parameters as in Table S1, footnote) could not reproduce the expected effects of 5-fold plasma dilution on thrombin generation (see Ref. [8]) in the presence of thrombomodulin. This suggested the necessity for further parameter adjustment, which is typically expected when an integrated kinetic model is assembled from independent "parts" (see, e.g., [3, 9]). These additional adjustments were made via the following procedure, which was based on the randomization of parameters k_{61}−k_{77} and k_{80}. We chose to adjust these specific parameters because they determine the rates of biochemical mechanisms involved in protein C/thrombomodulin system activity (Table S1), and our dilution modeling indicated that these particular mechanisms may need an improved representation in the model.

We generated 2000 random sets of values for parameters k_{61}−k_{77} and k_{80}. Each parameter was sampled independently from a log-uniform distribution over an interval that allowed for up to 3-fold changes with respect to the original parameter value. (Because it is rather common that biochemical reaction rates measured using distinct *in vitro* setups in different laboratories differ by 2−3 fold [10], such adjustments would not result in unrealistically high or low parameter values.) For each of the 2000 parameter sets, we ran our model to simulate thrombin curves for undiluted and diluted blood plasma (thrombin generation was simulated for a 40-min time interval with 2 pM initial TF; plasma dilution was 5 fold). We filtered out the parameter sets that resulted in unexpected shapes of thrombin curves (such as, curves having more than one peak or curves that did not reach 10 nM thrombin in 40 min). We also filtered out parameter sets for which thrombin peak height in diluted plasma was >70% of the thrombin peak height in non-diluted plasma. Of the remaining sets, we chose the one that gave the largest dilution-induced time delay for the thrombin peak. Such choice of parameter set made the dilution behavior of our model consistent with that of the core Hockin−Mann model of thrombin generation, which we investigated in an earlier study [8].

Table S1. Biochemical reactions and their parameters represented in the kinetic model. The notation $-k_x>$ (adopted from Ref. [3]) designates a forward reaction (with rate constant k_x), whose rate is defined by mass action law. The notation $<k_x–k_y>$ designates a reversible mass-action reaction, where the forward half-reaction has the rate constant k_y, and the reverse half-reaction has the rate constant k_x. The values of rate constants for forward reactions are also designated as k_+, whereas those for reverse reactions are designated as k_+. For complex reactions with three constituent simple reactions, the 2nd forward rate constant is denoted k_{cat}. The notation $-r_x>$ indicates a non-mass-action forward reaction with rate r_x, the expression for which is given in the footnote. The symbol ":" designates complex formation. References indicate the literature sources for distinct reaction mechanisms. For simple monomolecular and bimolecular reactions, the rate constants are expressed in units of s^{-1} and $M^{-1}\cdot s^{-1}$, respectively. The references for rate constant values are given in the footnote.

Line	Chemical reaction	k_+	$k_–$	k_{cat}	References
1	TF + FVII $<k_1–k_2>$ TF:FVII	3.2×10^{6}	3.1×10^{-3}		[3, 11]
2	TF + FVIIa $<k_3–k_4>$ TF:FVIIa	2.3×10^{7}	3.1×10^{-3}		[3, 11]
3	TF:FVIIa + FVII $–k_5>$ TF:FVIIa + FVIIa	4.4×10^{5}			[3, 11]
4	FXa + FVII $–k_6>$ FXa + FVIIa	1.3×10^{7}			[3, 11]
5	FIIa + FVII $–k_7>$ FIIa + FVIIa	2.3×10^{4}			[3, 11]
6	TF:FVIIa + FX $<k_8–k_9>$ TF:FVIIa:FX $–k_{10}>$ TF:FVIIa:FXa	2.5×10^{7}	1.05	6.0	[3, 11]
7	TF:FVIIa + FXa $<k_{11}–k_{12}>$ TF:FVIIa:FXa	2.2×10^{7}	19.0		[3, 11]
8	TF:FVIIa + FIX $<k_{13}–k_{14}>$ TF:FVIIa:FIX $–k_{15}>$ TF:FVIIa + FIXa	1.0×10^{7}	2.4	1.8	[3, 11]
9	FXa + FII $–k_{16}>$ FXa + FIIa	7.5×10^{3}			[3, 11]
10	FIIa + FVIII $–k_{17}>$ FIIa + FVIIIa	2.0×10^{7}			[3, 11]
11	FVIIIa + FIXa $<k_{18}–k_{19}>$ FIXa:FVIIIa	1.0×10^{7}	5.0×10^{-3}		[3, 11]
12	FIXa:FVIIIa + FX $<k_{20}–k_{21}>$ FIXa:FVIIIa:FX $–k_{22}>$ FIXa:FVIIIa + FXa	1.0×10^{8}	1.0×10^{-3}	8.2	[3, 11]
13	FVIIIa $<k_{23}–k_{24}>$ $FVIIIa_1$-L + $FVIIIa_2$	6.0×10^{-3}	2.2×10^{4}		[3, 11]
14	FIXa:FVIIIa:FX $–k_{25}>$ $FVIIIa_1$-L + $FVIIIa_2$ + FX + FIXa	1.0×10^{-3}			[3, 11]
15	FIXa:FVIIIa $–k_{25}>$ $FVIIIa_1$-L + $FVIIIa_2$ + FIXa	1.0×10^{-3}			[3, 11]
16	FIIa + FV $–k_{26}>$ FIIa + FVa	2.0×10^{7}			[3, 11]
17	FXa + FVa $<k_{27}–k_{28}>$ FXa:FVa	4.0×10^{8}	0.2		[3, 11]
18	FXa:FVa + FII $<k_{29}–k_{30}>$ FXa:FVa:FII $–k_{31}>$ FXa:FVa + mIIa	1.0×10^{8}	103.0	63.5	[3, 11]
19	mIIa + FXa:FVa $–k_{32}>$ FIIa + FXa:FVa	2.3×10^{8}			[3, 11]
20	FXa + TFPI $<k_{33}–k_{34}>$ FXa:TFPI	9.0×10^{5}	3.6×10^{-4}		[3, 11]
21	TF:FVIIa:FXa + TFPI $<k_{35}–k_{36}>$ TF:FVIIa:FXa:TFPI	3.2×10^{8}	1.1×10^{-4}		[3, 11]
22	TF:FVIIa + FXa:TFPI $–k_{37}>$ TF:FVIIa:FXa:TFPI	5.0×10^{7}			[3, 11]
23	FXa + AT $–k_{38}>$ FXa:AT	4.2×10^{3}			[3, 11]
24	mIIa + AT $–k_{39}>$ mIIa:AT	7.1×10^{3}			[3, 11]
25	FIXa + AT $–k_{40}>$ FIXa:AT	4.9×10^{2}			[3, 11]
26	FIIa + AT $–k_{41}>$ FIIa:AT	1.6×10^{4}			[3, 4, 11]
27	TF:FVIIa + AT $–k_{42}>$ TF:FVIIa:AT	2.3×10^{2}			[3, 11]
28	FIXa + FX $–k_{43}>$ FIXa + FXa	5.7×10^{3}			[11]
29	mIIa + FV $–k_{44}>$ mIIa + FVa	3.0×10^{6}			[11]
30	Fg + FIIa $<k_{45}–k_{46}>$ Fg:FIIa $–k_{47}>$ FnI + FIIa + FPA	1.0×10^{8}	7.2×10^{2}	84.0	[4]
31	FnI + FIIa $<k_{48}–k_{46}>$ FnI:FIIa $–k_{49}>$ FnII + FIIa + FPB	1.0×10^{8}	7.5×10^{2}	7.4	[4]
32	2FnI $<k_{50}–k_{51}>$ $(FnI)_2$	1.0×10^{6}	0.064		[4]
33	$(FnI)_2$ + FIIa $<k_{52}–k_{46}>$ $(FnI)_2$:FIIa $–k_{53}>$ $(FnII)_2$ + FIIa + 2FPB	1.0×10^{8}	7.5×10^{2}	49.0	[4]
34	FnII + FIIa $<k_{54}–k_{46}>$ FnII:FIIa	1.0×10^{8}	1.0×10^{3}		[4]
35	$(FnI)_2$:FIIa + AT $–k_{55}>$ $(FnI)_2$:FIIa:AT	1.6×10^{4}			[4]
36	FnI:FIIa + AT $–k_{55}>$ FnI:FIIa:AT	1.6×10^{4}			[4]
37	FnII:FIIa + AT $–k_{56}>$ FnII:FIIa:AT	1.0×10^{4}			[4]
38	Pn + AP $–k_{57}>$ Pn:AP	3.0×10^{6}			[5]
39	tPA + PAI $–k_{58}>$ tPA:PAI	4.0×10^{7}			[12]
40	Pg $–r_1>$ Pn (see footnote)	---			[6]
41	FnII $–r_2>$ FDP (see footnote)	---			[2]
42	$(FnII)_2$ $–r_3>$ 2FDP (see footnote)	---			[2]
43	Tm + FIIa $<k_{61}–k_{62}>$ Tm:FIIa	8.038×10^{7}	4.628×10^{-1}		[7]
44	Tm:FIIa + PC $<k_{63}–k_{64}>$ Tm:FIIa:PC $–k_{65}>$ Tm:FIIa + APC	3.377×10^{7}	2.026×10^{2}	2.545×10^{-1}	[7]
45	Tm:FIIa + AT $–k_{66}>$ FIIa:AT + Tm	1.495×10^{4}			[7]
46	APC + FVa $<k_{67}–k_{68}>$ APC:FVa	3.426×10^{7}	2.012×10^{0}		[7]
47	APC:FVa $–k_{69}>$ APC + FVa5	4.4×10^{-1}			[7]

48	APC:FVa $-k_{70}>$ APC + FVa3	1.381×10^{-1}			[7]
49	APC + FVa5 $<k_{67}-k_{68}>$ APC:FVa5 $-k_{70}>$ APC + FVa53	3.426×10^{7}	2.012×10^{0}	1.381×10^{-1}	[7]
50	APC + FVa3 $<k_{67}-k_{68}>$ APC:FVa3 $-k_{69}>$ APC + FVa53	3.426×10^{7}	2.012×10^{0}	4.4×10^{-1}	[7]
51	FVa3 $-k_{71}>$ HCF + LCA1	1.25×10^{-2}			[7]
52	FVa53 $-k_{71}>$ HCF + LCA1	1.25×10^{-2}			[7]
53	APC + LCA1 $<k_{67}-k_{68}>$ APC:LCA1	3.426×10^{7}	2.012×10^{0}		[7]
54	APC + Tm:FIIa $<k_{63}-k_{64}>$ Tm:FIIa:APC	3.377×10^{7}	2.026×10^{2}		[7]
55	FXa + FVa5 $<k_{72}-k_{28}>$ FXa:FVa5	4.0×10^{8}	2.947×10^{-1}		[7]
56	FXa + FVa3 $<k_{72}-k_{28}>$ FXa:FVa3	4.0×10^{8}	2.947×10^{-1}		[7]
57	FXa:FVa5 + FII $<k_{29}-k_{30}>$ FXa:FVa5:FII $-k_{73}>$ FXa:FVa5 + mIIa	1.0×10^{8}	103.0	2.369×10^{1}	[7]
58	FXa:FVa3 + FII $<k_{29}-k_{30}>$ FXa:FVa3:FII $-k_{74}>$ FXa:FVa3 + mIIa	1.0×10^{8}	103.0	5.994×10^{0}	[7]
59	FXa:FVa5 + mIIa $-k_{75}>$ FXa:FVa5 + FIIa	1.317×10^{8}			[7]
60	FXa:FVa3 + mIIa $-k_{76}>$ FXa:FVa3 + FIIa	1.042×10^{8}			[7]
61	FXa:FVa3 $-k_{77}>$ HCF + LCA1 + FXa	2.93×10^{-3}			[7]
62	FXa:FVa3:FII $-k_{77}>$ HCF + LCA1 + FXa + FII	2.93×10^{-3}			[7]
63	Tm + mIIa $<k_{61}-k_{62}>$ Tm:mIIa	8.038×10^{7}	4.628×10^{-1}		[7]
64	Tm:mIIa + PC $<k_{63}-k_{64}>$ Tm:mIIa:PC $-k_{65}>$ Tm:mIIa + APC	3.377×10^{7}	2.026×10^{2}	2.545×10^{-1}	[7]
65	Tm:mIIa + AT $-k_{66}>$ mIIa:AT + Tm	1.495×10^{4}			[7]
66	FXa + FVa53 $<k_{72}-k_{28}>$ FXa:FVa53	4.0×10^{8}	2.947×10^{-1}		[7]
67	FXa:FVa53 + FII $<k_{29}-k_{30}>$ FXa:FVa53:FII $-k_{74}>$ FXa:FVa53 + mIIa	1.0×10^{8}	103.0	5.994×10^{0}	[7]
68	FXa:FVa53 + mIIa $-k_{76}>$ FXa:FVa53 + FIIa	1.042×10^{8}			[7]
69	FXa:FVa53 $-k_{77}>$ HCF + LCA1 + FXa	2.93×10^{-3}			[7]
70	FXa:FVa53:FII $-k_{77}>$ HCF + LCA1 + FXa + FII	2.93×10^{-3}			[7]
71	FII + FVa $<k_{78}-k_{79}>$ FII:FVa	3.33×10^{7}	210.0		[7]
72	FXa:FVa5 + APC $-k_{80}>$ FXa:FVa53 + APC	1.707×10^{6}			[7]

The values of the rate constants k_1–k_{31}, k_{33}–k_{37}, k_{39}, k_{40}, and k_{42} were taken from Refs. [3, 11]; the values for the rate constants k_{32}, k_{38}, k_{43}, and k_{44} were taken from Ref. [11]; the values for k_{41}, k_{47}, k_{49}–k_{51}, k_{53}, and k_{55}–k_{56} were taken from Ref. [4]. The value of k_{46} was taken from Ref. [13]. The values of k_{45}, k_{48}, k_{52}, and k_{54} were calculated from the value of k_{46} and the corresponding equilibrium constants in Ref. [4]. Our value for k_{57} is based on Ref. [5]. The value of k_{58} is the value for plasmin-cleaved (i.e., single-chain) tPA from Ref. [12]. Our values for k_{61}–k_{80} were modified from Ref. [7] (see *Parameter selection*).

The non-mass-action rates r_1–r_3 (*Lines 40–42* in the Table) were defined as follows:

$$r_1 = \frac{k_{59}[\mathrm{tPA}][\mathrm{Pg}][C_{\mathrm{FnII}}]/(K_1 + C_{\mathrm{FnII}})}{[\mathrm{Pg}] + K_2(K_3 + C_{\mathrm{FnII}})/(K_1 + C_{\mathrm{FnII}})}, \quad \text{where } C_{\mathrm{FnII}} = [\mathrm{FnII}] + 2[(\mathrm{FnII})_2];$$

$$r_2 = \frac{k_{60}[\mathrm{Pn}][\mathrm{FnII}]}{K_4 + [\mathrm{FnII}]};$$

$$r_3 = \frac{k_{60}[\mathrm{Pn}][(\mathrm{FnII})_2]}{K_4 + [(\mathrm{FnII})_2]}.$$

In these expressions, $k_{59} = 0.09\ \mathrm{s}^{-1}$ (modified from Ref. [6]; see *Parameter selection*); $k_{60} = 0.47\ \mathrm{s}^{-1}$ [2]; $K_1 = 7.7\times10^{-8}$ M, $K_2 = 4.1\times10^{-7}$ M, $K_3 = 3.0\times10^{-7}$ M [6], and $K_4 = 2.1\times10^{-6}$ M [2].

Table S2. Initial concentrations of coagulation factors in the kinetic model. All the chemical species not listed in this table have zero initial concentrations.*

Protein factor	Concentration (M)	Reference
TF	Varied	[3]
FVII	1.0×10^{-8}	[3]
FVIIa	1.0×10^{-10}	[3]
FX	1.6×10^{-7}	[3]
FIX	9.0×10^{-8}	[3]
FII	1.4×10^{-6}	[3]
FVIII	7.0×10^{-10}	[3]
FV	2.0×10^{-8}	[3]
TFPI	2.5×10^{-9}	[3]
AT	3.4×10^{-6}	[3]
Fg	9.0×10^{-6}	[14]
Pg	2.0×10^{-6}	[15]
PAI	4.0×10^{-10}	[15]
AP	1.0×10^{-6}	[15]
tPA	7.0×10^{-11}	[15]
PC	7.0×10^{-8}	[16]
Tm	1.0×10^{-9}	[7]
TAFI	7.5×10^{-8}	[15]

*The initial concentrations represent the mean levels of coagulation factors in normal human plasma.

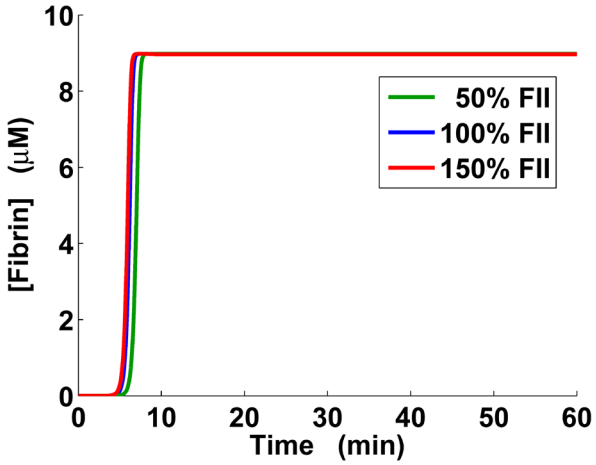

Fig. S1. Dependence of fibrin generation on the initial prothrombin concentration. "FII" designates prothrombin, whose level is expressed as percentage of the mean normal prothrombin level in human plasma (i.e., 1.4 μM). Thrombin generation was initiated with 5 pM tissue factor (TF); all other initial concentrations were as in the simulations shown in Fig. 2*A*, with 9.0 μM initial fibrinogen.

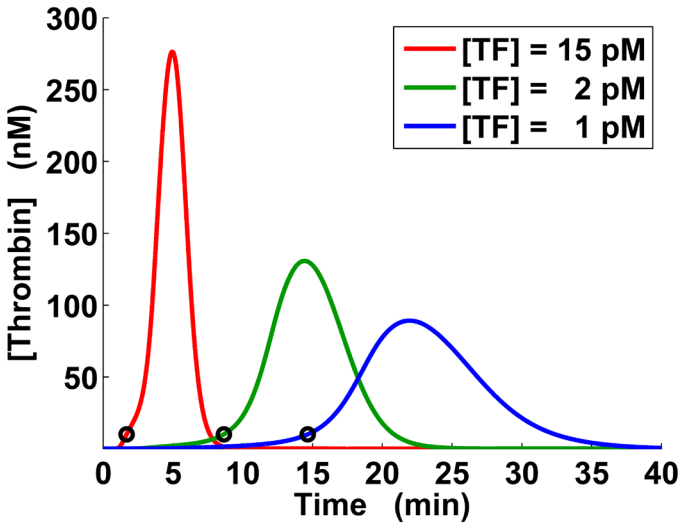

Fig. S2. Tissue factor concentration impacts the kinetics of thrombin formation. Model-predicted thrombin generation at different TF levels. Circle markers designate the thrombin trajectory points corresponding to clotting time (i.e., the time when thrombin concentration reaches 10 nM). The initial conditions were the same as for the simulations shown in Fig. 4*A*.

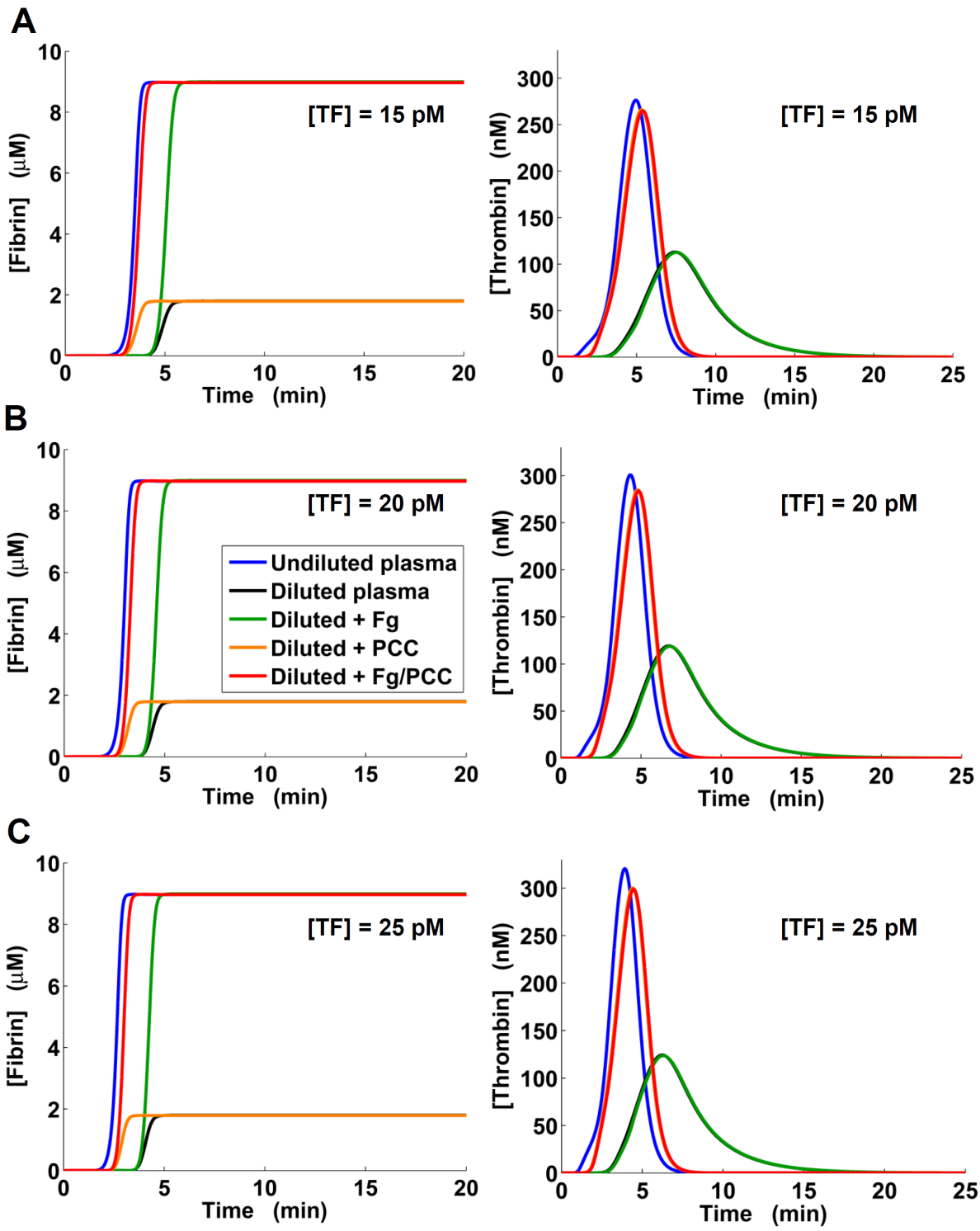
A
[Fibrin] (μM)
[TF] = 15 pM
Time (min)
[Thrombin] (nM)
[TF] = 15 pM
Time (min)
B
[Fibrin] (μM)
[TF] = 20 pM
Undiluted plasma
Diluted plasma
Diluted + Fg
Diluted + PCC
Diluted + Fg/PCC
Time (min)
[Thrombin] (nM)
[TF] = 20 pM
Time (min)
C
[Fibrin] (μM)
[TF] = 25 pM
Time (min)
[Thrombin] (nM)
[TF] = 25 pM
Time (min)

Fig. S3. Kinetic modeling of the restoration of normal thrombin and fibrin generation in diluted plasma by clotting factor supplementation. “Fg” stands for supplementation with fibrinogen, “PCC” denotes supplementation with PCC-AT (i.e., a combination of the factors II, IX, X, and antithrombin), and “Fg/PCC” denotes simultaneous supplementation with fibrinogen and PCC-AT. *A*: Clotting was initiated with 15 pM TF. *B*: Clotting was initiated with 20 pM TF. *C*: Clotting was initiated with 25 pM TF. The orange and red lines, as well as black and green lines, coincide for thrombin generation.

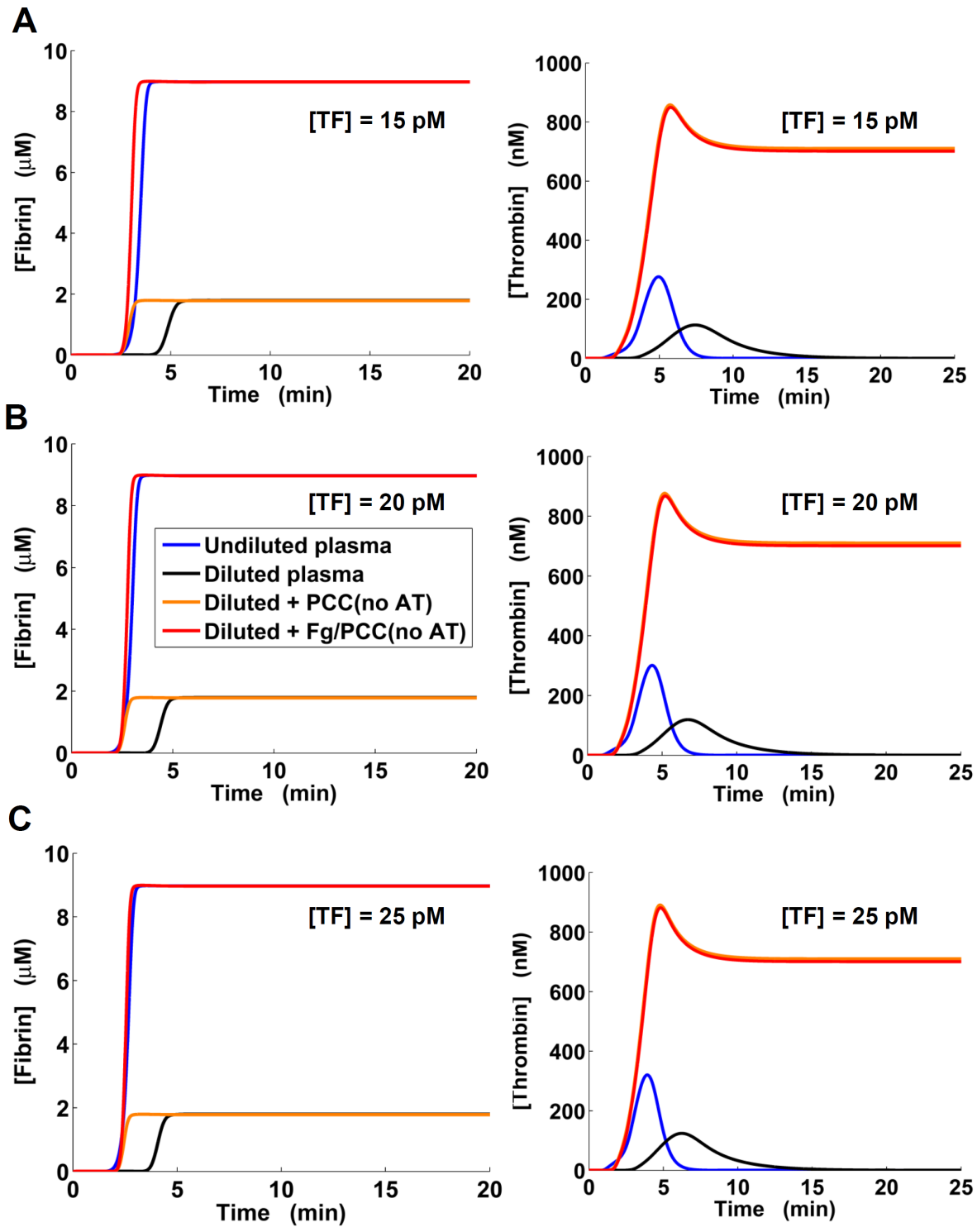
A
[Fibrin] (μM)
[TF] = 15 pM
Time (min)
[Thrombin] (nM)
[TF] = 15 pM
Time (min)
B
[Fibrin] (μM)
[TF] = 20 pM
Undiluted plasma
Diluted plasma
Diluted + PCC(no AT)
Diluted + Fg/PCC(no AT)
Time (min)
[Thrombin] (nM)
[TF] = 20 pM
Time (min)
C
[Fibrin] (μM)
[TF] = 25 pM
Time (min)
[Thrombin] (nM)
[TF] = 25 pM
Time (min)

Fig. S4. Model-predicted effects of supplementing diluted plasma with the three procoagulant PCC components (i.e., factors II, IX, and X) with and without fibrinogen; no antithrombin was added. The PCC component supplementation is denoted "PCC(No AT)" without fibrinogen and "Fg/PCC(No AT)" with fibrinogen. *A*: Clotting was initiated with 2 pM TF. *B*: Clotting was initiated with 5 pM TF. *C*: Clotting was initiated with 10 pM TF.

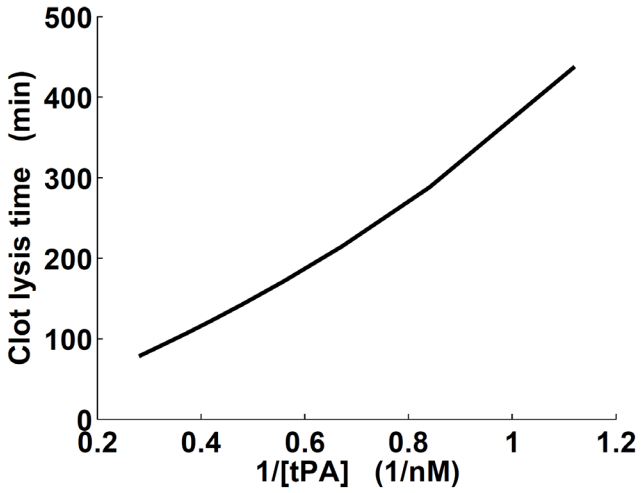

Fig. S5. Kinetic modeling of the dependence of clot lysis time on the concentration of tPA in the absence of TAFI. The clots were pre-formed for 30 min, then lysis was initiated at time 0 by adding tPA (on the *x*-axis, shown is the inverse of the total tPA concentration). Clot lysis was monitored for 700 min.

References

[1] Mitrophanov AY, Reifman J. Kinetic modeling sheds light on the mode of action of recombinant factor VIIa on thrombin generation. Thromb Res. 2011;128:381-90.
[2] Kim PY, Stewart RJ, Lipson SM, Nesheim ME. The relative kinetics of clotting and lysis provide a biochemical rationale for the correlation between elevated fibrinogen and cardiovascular disease. J Thromb Haemost. 2007;5:1250-6.
[3] Hockin MF, Jones KC, Everse SJ, Mann KG. A model for the stoichiometric regulation of blood coagulation. J Biol Chem. 2002;277:18322-33.
[4] Naski MC, Shafer JA. A kinetic model for the α-thrombin-catalyzed conversion of plasma levels of fibrinogen to fibrin in the presence of antithrombin III. J Biol Chem. 1991;266:13003-10.
[5] Schneider M, Brufatto N, Neill E, Nesheim M. Activated thrombin-activatable fibrinolysis inhibitor reduces the ability of high molecular weight fibrin degradation products to protect plasmin from antiplasmin. J Biol Chem. 2004;279:13340-5.
[6] Horrevoets AJG, Pannekoek H, Nesheim ME. A steady-state template model that describes the kinetics of fibrin-stimulated [Glu^1]- and [Lys^1]-plasminogen activation by native tissue-type plasminogen activator and variants that lack either the finger or kringle-2 domain. J Biol Chem. 1996;272:2183-91.
[7] Brummel-Ziedins KE, Orfeo T, Callas PW, Gissel M, Mann KG, Bovill EG. The prothrombotic phenotypes in familial protein C deficiency are differentiated by computational modeling of thrombin generation. PLOS ONE. 2012;7:e44378.
[8] Mitrophanov AY, Rosendaal FR, Reifman J. Computational analysis of intersubject variability and thrombin generation in dilutional coagulopathy. Transfusion. 2012;52:2475-86.
[9] Baugh RJ, Broze GJ, Jr., Krishnaswamy S. Regulation of extrinsic pathway factor Xa formation by tissue factor pathway inhibitor. J Biol Chem. 1998;273:4378-86.
[10] Bravo MC, Orfeo T, Mann KG, Everse SJ. Mathematical modeling of human factor Va inactivation by activated protein C. BMC Syst Biol. 2012;6:45.
[11] Danforth CM, Orfeo T, Mann KG, Brummel-Ziedins KE, Everse SJ. The impact of uncertainty in a blood coagulation model. Math Med Biol. 2009;26:323-36.
[12] Heckman CM, Loskutoff DJ. Kinetic analysis of the interactions between plasminogen activator inhibitor 1 and both urokinase and tissue plasminogen activator. Arch Biochem Biophys. 1988;262:199-210.
[13] Chatterjee MS, Denney WS, Jing H, Diamond SL. Systems biology of blood coagulation initiation: kinetics of thrombin generation in resting and activated human blood. PLOS Comp Biol. 2010;6:e1000950.
[14] Brummel KE, Butenas S, Mann KG. An integrated study of fibrinogen during blood coagulation. J Biol Chem. 1999;274:22862-70.
[15] Rijken DC, Lijnen HR. New insights into the molecular mechanisms of the fibrinolytic system. J Thromb Haemost. 2009;7:4-13.
[16] Mosnier LO, Zlokovic BV, Griffin JH. The cytoprotective protein C pathway. Blood. 2007;109:3161-72.